Available online at www.sciencedirect.com
SCIENCE @ DIRECT®

Journal of Magnetic Resonance 171 (2004) 15–19

JMR
Journal of
Magnetic Resonance

www.elsevier.com/locate/jmr

Switching-angle sample spinning NMR probe with a commercially available 20 kHz spinning system

Takashi Mizuno*, K. Takegoshi, Takehiko Terao

Department of Chemistry, Graduate School of Science, Kyoto University, Kyoto 606-8502, Japan

Received 8 June 2004; revised 21 July 2004
Available online 23 August 2004

Abstract

A switching-angle sample spinning (SASS) probe workable at high spinning speeds was developed using a commercially available rotor/housing system. Details of the construction are described. As application examples of the SASS probe, we report experiments of powder pattern separation at the spinning speed of 20 kHz and broadband ^{13}C–^{13}C polarization transfer at 16 kHz.

Keywords: Probe; SASS

---

1. Introduction

In solid-state NMR, measurements of anisotropic interactions provide plenty of information on static and dynamic structures of molecules. Accordingly, a variety of methods to measure anisotropies have been developed. Switching-angle sample spinning (SASS), which is one of such methods, enables us to separately observe individual powder patterns of chemically distinct nuclei, using a two-dimensional (2D) NMR scheme with the rotor orientation along an off-magic angle during the evolution period and the magic angle during the detection period. The 1D version of SASS has also been performed using a selective rf-pulse [1,2]. Powder patterns due to chemical-shift anisotropy (CSA) [3,4], ^{13}C–^{1}H dipolar [5], and ^{13}C–^{13}C dipolar interactions [6] have been separately observed by 2D or 1D SASS for studies of the conformations of inclusion compounds [7–9], the motions of glassy polymers [10,11], and the orientation-ordering of liquid crystal [12]. Another powerful approach to recover anisotropic interactions is rotor-synchronized rf-pulse sequences, which have been developed to recover CSA [13,14], ^{13}C–^{1}H dipolar [15,16], and ^{13}C–^{13}C dipolar [17] interactions under magic angle spinning (MAS). These sequences are sensitive to pulse imperfections such as rf-field inhomogeneity, finite pulse width, and resonance offset, while SASS is free from such rf imperfections at least in separation of overlapped CSA powder patterns. Furthermore, MAS frequency usable in the rotor-synchronous pulse sequences is usually limited to ~5 kHz, although a few trials have been reported to raise the limitation to somewhat higher frequency [18,19]. In general, however, fast MAS is required both for obtaining sideband-free spectra in high magnetic fields and for removing ^{13}C–^{13}C dipolar broadening in uniformly ^{13}C-labeled samples. Although SASS experiments have been made at relatively low speeds (<10 kHz), there should be no limit to the MAS frequency in principle. In this work, instead of improving spinning speed in the published probe designs [20,21], we built a SASS probe workable at high-spinning speeds utilizing a commercially available rotor/housing system. The blueprints of the probe are available on request.

As shown in Fig. 1, the probe system was constructed by adding upper and lower attachments to a commercially available probe: DSI-692 Doty Co. The height of

---

[*] Corresponding author. Present address: JEOL Ltd., 1-2 Musashino 3-Chome Akishima Tokyo 196-8558, Japan.
E-mail address: tmizuno@jeol.co.jp (T. Mizuno).

1090-7807/$ - see front matter © 2004 Elsevier Inc. All rights reserved.
doi:10.1016/j.jmr.2004.07.014

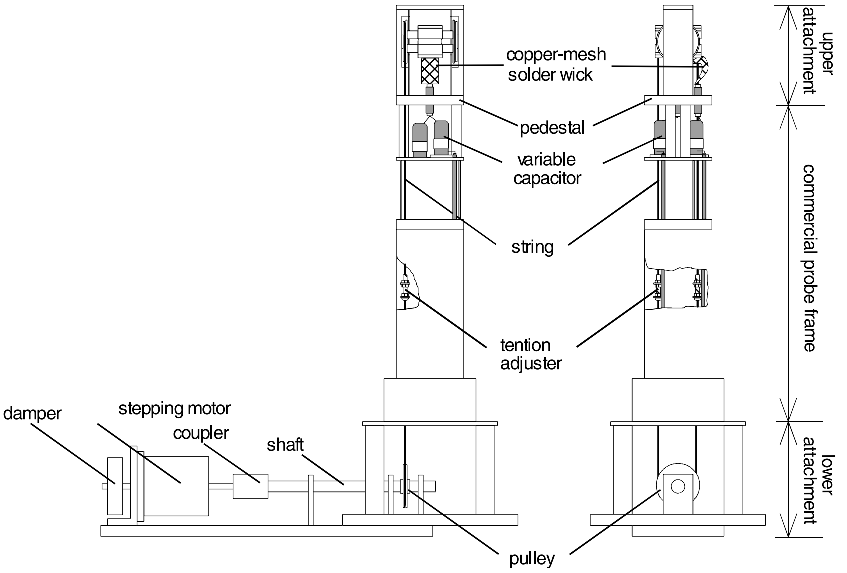

Fig. 1. The whole sketch of the SASS NMR probe. The upperside of the probe is drawn with the cover taken off.

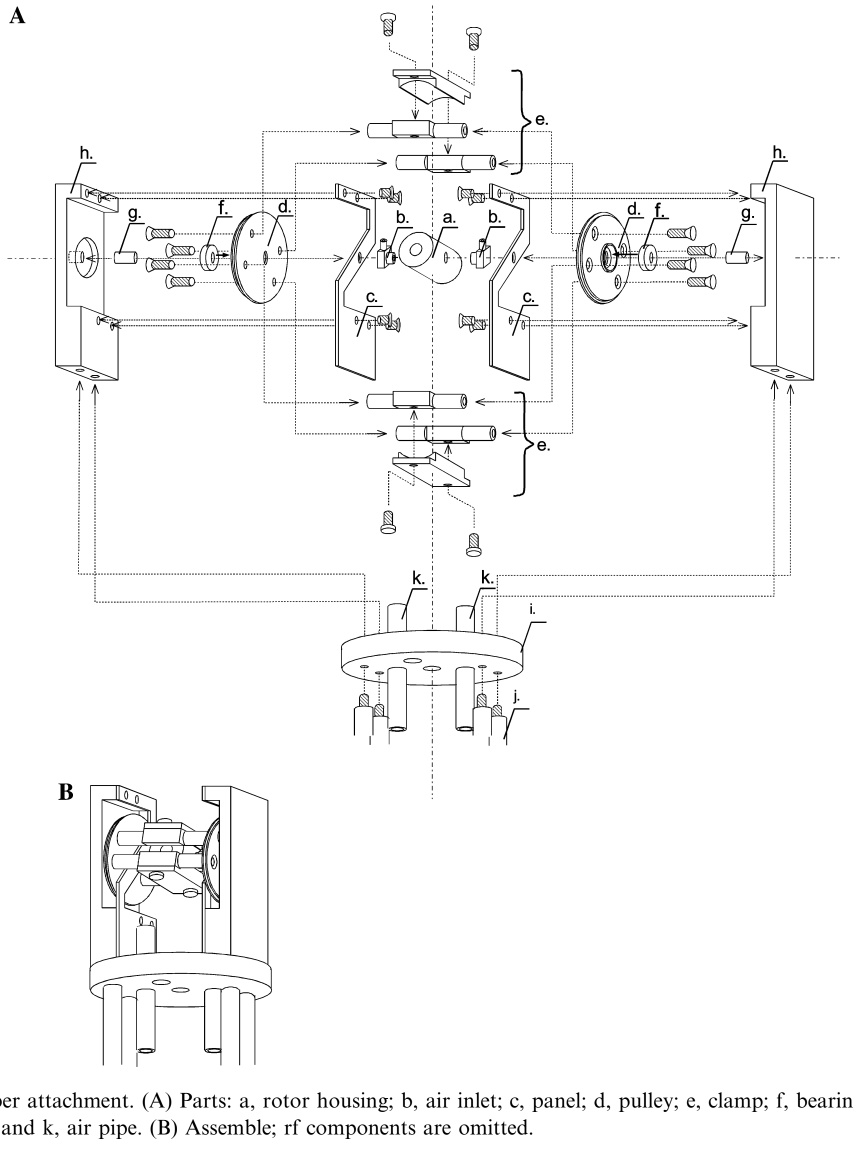

Fig. 2. Sketches of the upper attachment. (A) Parts: a, rotor housing; b, air inlet; c, panel; d, pulley; e, clamp; f, bearing; g, pulley axis; h, pulley holder; i, pedestal; j, prop; and k, air pipe. (B) Assemble; rf components are omitted.

the whole probe is short enough to enter the space under the magnet. The upper attachment, which is illustrated in Fig. 2, is composed of the movable assembly (a, b, d, e, f, in Fig. 2A) and the fixed assembly (c, g, h, i, j, in Fig. 2A). In the former, pair of pulleys with a bearing and a clamp firmly hold a commercial rotor/housing system with air inlets (Vespel; DuPond). Most of commercially available rotor/housing systems can be incorporated by slightly modifying the lower and upper clamps. In fact, we could incorporate a Doty 5 mm rotor/housing system (max spinning speed: ~14 kHz) and a Chemagnetics 3.2 mm rotor/housing system (max spinning speed: ~20 kHz). The solenoid coils in these commercial rotor/housing systems were used as they are. In the fixed assembly, pair of pulley holders with a panel (Duracon; Polyplastics), and a pulley axis (Vespel) are fixed on a brass pedestal supported on the top of a Doty DSI probe by four duralumin props. The movable assembly is supported by the fixed assembly via the connection of the pulley axis and the bearing. Thus, the orientation of the spinner axis can be changed around the pulley axes, where the zigzag shape of the panels restricts the range of the angle between the spinner axis and the magnetic field to 20°–90°. The range can be expanded, for example to 0°–90°, by modifying the shape of the panel. The compressed air for sample spinning is supplied with the air inlets via the flexible silicon tubes. We connected each end of the sample coil with a different tuning-capacitor via a flexible wire (three pieces of copper-mesh solder wick) and a semi-rigid cable. In practice, we confirmed that the solder wick pieces exhibit no signs of break after bending 1,000,000 times.

The lower attachment is composed of a pulley and a stepping motor system. The upper and lower pulleys are linked with each other by 0.5 mm-diameter high tensile-strength strings of Zylon (Toyobo) or Kevlar (DuPond). To adjust the tensile strength of the string, the tension adjuster with two polycarbonate bolts and acrylic nuts is used. We adopted a high-precession stepping motor system (Compumotor) for switching the spinner-axis, which includes a motor driver (Zeta-A4 driver) and a programmable motor controller (500-controller). The field gradient at the position of the stepping motor should be small enough not to cause motor malfunction. We used a motor shaft of ca. 35 cm long ca. 12 cm below the bottom of the magnet to set the motor at a proper position. The motor driver has a resolution of 0.0072° per step with the settling time shorter than 7 ms. Angle-switching sequence programs are written in the controller, which can be executed synchronously with a pulse sequence by applying a trigger signal. We found that the angle switching of ca. 20° takes about 40 ms for keeping spinning speed stable within the accuracy of ±0.01 kHz at a spinning speed of 20 kHz.

NMR experiments were carried out with the ^{13}C resonance frequency of 100.65 MHz at room temperature by using a Chemagnetics CMX-400 spectrometer and the present SASS probe system with a Chemagnetics 3.2 mm rotor/housing system to demonstrate the performance of the probe.

We firstly made a 2D SASS NMR experiment for ^{13}C CSA powder pattern separation in dimedone (5,5-dimethyl-1,3-cyclohexanedione) under the spinning speed of 20.07 kHz and $\theta_{\text{off}} = 67.0°$ using the pulse sequence shown in Fig. 3A. This spinning speed ensures observation of spinning sideband-free spectra. The observed and simulated powder patterns are shown in Fig. 3B for the

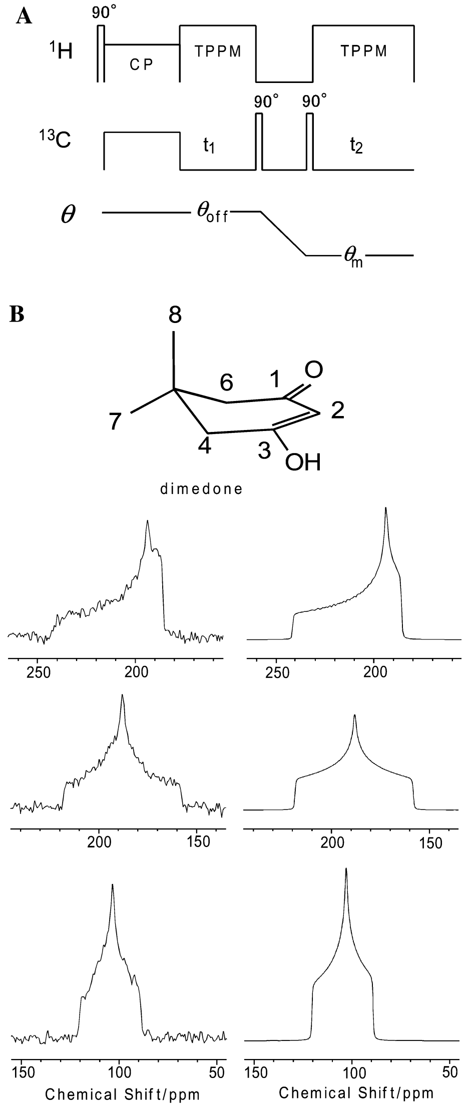

Fig. 3. 2D SASS NMR separation of ^{13}C CSA powder patterns. (A) Pulse sequence. (B) Separated ^{13}C powder patterns for C1 (top), C3 (middle), and C2 (bottom)in dimedone. Left side: observed spectra under the spinning speed of 20.07 ± 0.01 kHz and $\theta_{\text{off}} = 67.0°$. 128 FIDs with 512 t_1 points were accumulated. The CP contact time was 3 ms and ^{1}H TPPM decoupling [22] was applied with 92 kHz nutation intensity and ±20° phase alternation. Right side: simulated spectra using the reported chemical-shift principal values (δ_{11}, δ_{22}, and δ_{33}) in ppm relative to TMS: C1 (284.1, 254.9, and 79.0); C3 (298.2, 188.0, and 75.6); and C2 (158.4, 107.7, and 43.3) [23].

carbons of C1, C3, and C2. The simulated powder patterns were obtained by using the reported chemical shift principal values [23], well reproducing the experimental spectra. The curve of the solder wick pieces was adjusted so that the ^{1}H channel could be tuned at the magic angle (θ_m) and 67.0° simultaneously. Then, the ^{1}H channel is slightly off-tuned at the other off-magic angles. On the other hand, we found that the tuning of the ^{13}C channel is almost independent of the rotor orientation.

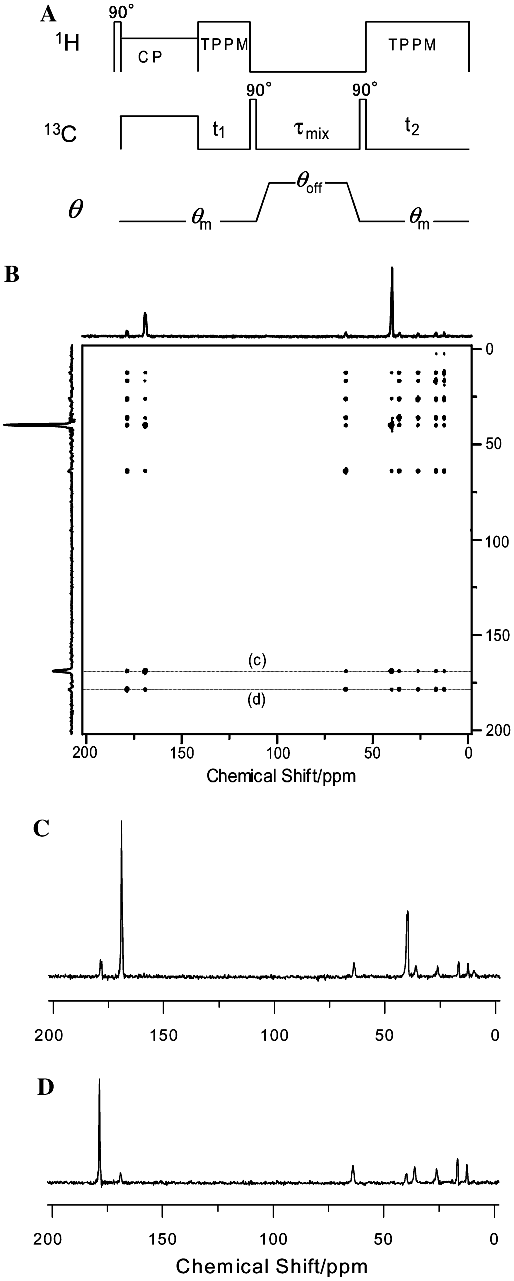

Fig. 4. ^{13}C–^{13}C SASS polarization transfer experiments. (A) Pulse sequence. (B) ^{13}C–^{13}C 2D NMR spectrum for [^{13}C, ^{15}N]glycilisoleucine under the spinning speed of 16.000 ± 0.005 kHz and $\theta_{off} = 40.5°$. FIDs (64) with 256 t_1 points were accumulated. (C and D) 1D cross-section spectra at the dotted lines in (B).

As another application example of the SASS probe, a broadband ^{13}C–^{13}C polarization transfer experiment was performed in uniformly [^{13}C, ^{15}N]-labeled glycilisoleucine under the spinning speed of 16 kHz using the pulse sequence given in Fig. 4A. Broadening due to dipolar and CSA interactions induces the spectral overlap necessary for the polarization transfer during the mixing time. Fig. 4B shows a 2D exchange spectrum obtained with the mixing time of 120 ms and $\theta_{off} = 40.5°$. The cross peaks and cross-sections (Figs. 4C and D) clearly indicate that broadband ^{13}C–^{13}C polarization transfer takes place. It is in progress to examine the θ_{off} dependence as well as the mixing time dependence of the 2D spectrum to clarify whether these cross peak intensities are related to the corresponding ^{13}C–^{13}C distances.

Acknowledgment

This work was supported by the Grant-in-Aid for Scientific Research from the Ministry of Education, Culture, Sports, Science and Technology.

References

[1] J.H. Iwamiya, M.F. Davis, G.E. Maciel, A 1D FT experiment for obtaining chemical-shift tensors in complex solids, using selective excitation and flipping of the spinner axis, J. Magn. Reson. 88 (1990) 199–204.

[2] J. Ashida, T. Nakai, T. Terao, 1D NMR separation of overlapping powder patterns by selective rf irradiation and switching-angle spinning, Chem. Phys. Lett. 168 (1990) 523–528.

[3] T. Terao, T. Fujii, T. Onodera, A. Saika, in: A. Saika (Ed.), Proceedings of 22nd NMR Symposium, Kyoto, 1983, p. 22;
T. Terao, T. Fujii, T. Onodera, A. Saika, Switching-angle sample spinning NMR spectroscopy for obtaining powder-pattern resolved 2D spectra: measurements of ^{13}C chemical-shift anisotropies in powdered 3,4-dimethoxybenzaldehyde, Chem. Phys. Lett. 107 (1984) 145–148.

[4] A. Bax, N.M. Szeverenyi, G.E. Maciel, Chemical-shift anisotropy in powdered solids studied by 2D FT NMR with flipping of the spinning axis, J. Magn. Reson. 55 (1983) 494–497.

[5] T. Terao, H. Miura, A. Saika, Dipolar SASS NMR spectroscopy: separation of heteronuclear dipolar powder patterns in rotating solids, J. Chem. Phys. 85 (1986) 3816–3826.

[6] A.C. Kolbert, P.J. Grandinetti, M. Baldwin, S.B. Prusiner, A. Pines, Measurement of internuclear distances by switched angle spinning NMR, J. Phys. Chem. 98 (1994) 7936–7938.

[7] F. Imashiro, D. Kuwahara, T. Nakai, T. Terao, Study on conformations of *n*-alkanes in urea inclusion compounds using CH dipolar switching-angle sample spinning nuclear magnetic resonance and MM2 molecular mechanics calculations, J. Chem. Phys. 90 (1988) 3356–3362.

[8] F. Imashiro, D. Kuwahara, T. Terao, ^{13}C Solid-state NMR study on populations, conformations, and molecular motions of γ-valerolactone enantiomers enclathrated in the chiral cholic acid host, J. Chem. Soc. Perkin Trans. 2. (1993) 1759–1763.

[9] D. Kuwahara, F. Imashiro, T. Terao, Dynamics of ferrocene molecules enclathrated in β-cyclodextrin as studied by variable-temperature one-dimensional SASS (switching angle sample spinning) NMR spectroscopy, Chem. Phys. Lett. 204 (1993) 533–537.

[10] F. Horii, T. Beppu, N. Takaesu, M. Ishida, Selective excitation SASS ^{13}C NMR study of the phenylene motion of glassy polymers, Magn. Reson. Chem. 32 (1994) 30–35.

[11] H. Kaji, T. Tai, F. Horii, Two-dimensional solid-state NMR analyses of medium-range molecular motion of polymers, Proc. Soc. Solid-State NMR Mater. 21 (1997) 35–39.

[12] R.H. Havlin, G.H.J. Park, A. Pines, Two-dimensional NMR correlation of liquid crystals using switched angle spinning, J. Magn. Reson. 157 (2002) 163–169.

[13] R. Tycko, G. Dabbagh, P.A. Mirau, Determination of chemical-shift anisotropy lineshapes in a two-dimensional magic-angle-spinning NMR experiment, J. Magn. Reson. 85 (1989) 265–274.

[14] S.F. Liu, J.D. Mao, K. Schmidt-Rohr, A robust technique for two-dimensional separation of undistorted chemical-shift anisotropy powder patterns in magic-angle-spinning NMR, J. Magn. Reson. 155 (2002) 15–28.

[15] Y. Ishii, T. Terao, M. Kainosho, Relayed anisotropy correlation NMR: determination of dihedral angles in solids, Chem. Phys. Lett. 256 (1996) 133–140.

[16] K. Takegoshi, T. Terao, ^{13}C–^{1}H dipolar recoupling under very fast magic-angle spinning using virtual pulses, Solid State NMR 13 (1999) 203–212.

[17] A.E. Bennet, C.M. Rienstra, J.M. Griffiths, W. Zhen, P.T. Lansbury Jr., R.G. Griffin, Homonuclear radio frequency-driven recoupling in rotating solids, J. Chem. Phys. 108 (1998) 9463–9479.

[18] Y. Ishii, T. Terao, Manipulation of nuclear spin Hamiltonians by rf-field modulations and its applications to observation of powder patterns under magic-angle spinning, J. Chem. Phys. 109 (1998) 1366–1374.

[19] R. Witter, St. Hesse, U. Sternberg, Powder pattern recoupling at 10 kHz spinning speed applied to cellulose, J. Magn. Reson. 161 (2003) 35–42.

[20] K.T. Mueller, G.C. Chingas, A. Pines, NMR probe for dynamic-angle spinning, Rev. Sci. Instrum. 62 (1991) 1445–1452.

[21] F.D. Doty, G. Entzminger, Y.A. Yang, Magnetism in high-resolution NMR probe design. II: HR MAS, Concepts Magn. Reson. 10 (1998) 239–260.

[22] A.E. Bennet, C.M. Reinstra, M. Auger, K.V. Lakshmi, R.G. Griffin, Heteronuclear decoupling in rotating solids, J. Chem. Phys. 103 (1995) 6951–6958.

[23] K. Takegoshi, A. Naito, C.A. McDowell, Intermolecular hydrogen-bonding effects on the ^{13}C NMR shielding tensor of the carbonyl carbon nucleus in a single crystal of dimedone, J. Magn. Reson. 65 (1985) 34–42.